Measurements of Absolute Branching Fractions of Fourteen Exclusive Hadronic D Decays to η

M. Ablikim,[1] M. N. Achasov,[10,c] P. Adlarson,[64] S. Ahmed,[15] M. Albrecht,[4] A. Amoroso,[63a,63c] Q. An,[60,48] Anita,[21]
X. H. Bai,[54] Y. Bai,[47] O. Bakina,[29] R. Baldini Ferroli,[23a] I. Balossino,[24a] Y. Ban,[38,k] K. Begzsuren,[26] J. V. Bennett,[5]
N. Berger,[28] M. Bertani,[23a] D. Bettoni,[24a] F. Bianchi,[63a,63c] J. Biernat,[64] J. Bloms,[57] A. Bortone,[63a,63c] I. Boyko,[29]
R. A. Briere,[5] H. Cai,[65] X. Cai,[1,48] A. Calcaterra,[23a] G. F. Cao,[1,52] N. Cao,[1,52] S. A. Cetin,[51b] J. F. Chang,[1,48] W. L. Chang,[1,52]
G. Chelkov,[29,b] D. Y. Chen,[6] G. Chen,[1] H. S. Chen,[1,52] M. L. Chen,[1,48] S. J. Chen,[36] X. R. Chen,[25] Y. B. Chen,[1,48]
W. S. Cheng,[63c] G. Cibinetto,[24a] F. Cossio,[63c] X. F. Cui,[37] H. L. Dai,[1,48] J. P. Dai,[42,g] X. C. Dai,[1,52] A. Dbeyssi,[15]
R. B. de Boer,[4] D. Dedovich,[29] Z. Y. Deng,[1] A. Denig,[28] I. Denysenko,[29] M. Destefanis,[63a,63c] F. De Mori,[63a,63c] Y. Ding,[34]
C. Dong,[37] J. Dong,[1,48] L. Y. Dong,[1,52] M. Y. Dong,[1,48,52] S. X. Du,[68] J. Fang,[1,48] S. S. Fang,[1,52] Y. Fang,[1] R. Farinelli,[24a]
L. Fava,[63b,63c] F. Feldbauer,[4] G. Felici,[23a] C. Q. Feng,[60,48] M. Fritsch,[4] C. D. Fu,[1] Y. Fu,[1] X. L. Gao,[60,48] Y. Gao,[38,k] Y. Gao,[61]
Y. G. Gao,[6] I. Garzia,[24a,24b] E. M. Gersabeck,[55] A. Gilman,[56] K. Goetzen,[11] L. Gong,[37] W. X. Gong,[1,48] W. Gradl,[28]
M. Greco,[63a,63c] L. M. Gu,[36] M. H. Gu,[1,48] S. Gu,[2] Y. T. Gu,[13] C. Y. Guan,[1,52] A. Q. Guo,[22] L. B. Guo,[35] R. P. Guo,[40]
Y. P. Guo,[9,h] Y. P. Guo,[28] A. Guskov,[29] S. Han,[65] T. T. Han,[41] T. Z. Han,[9,h] X. Q. Hao,[16] F. A. Harris,[53] K. L. He,[1,52]
F. H. Heinsius,[4] T. Held,[4] Y. K. Heng,[1,48,52] M. Himmelreich,[11,f] T. Holtmann,[4] Y. R. Hou,[52] Z. L. Hou,[1] H. M. Hu,[1,52]
J. F. Hu,[42,g] T. Hu,[1,48,52] Y. Hu,[1] G. S. Huang,[60,48] L. Q. Huang,[61] X. T. Huang,[41] Y. P. Huang,[1] Z. Huang,[38,k] N. Huesken,[57]
T. Hussain,[62] W. Ikegami Andersson,[64] W. Imoehl,[22] M. Irshad,[60,48] S. Jaeger,[4] S. Janchiv,[26,j] Q. Ji,[1] Q. P. Ji,[16] X. B. Ji,[1,52]
X. L. Ji,[1,48] H. B. Jiang,[41] X. S. Jiang,[1,48,52] X. Y. Jiang,[37] J. B. Jiao,[41] Z. Jiao,[18] S. Jin,[36] Y. Jin,[54] T. Johansson,[64]
N. Kalantar-Nayestanaki,[31] X. S. Kang,[34] R. Kappert,[31] M. Kavatsyuk,[31] B. C. Ke,[43,1] I. K. Keshk,[4] A. Khoukaz,[57]
P. Kiese,[28] R. Kiuchi,[1] R. Kliemt,[11] L. Koch,[30] O. B. Kolcu,[51b,e] B. Kopf,[4] M. Kuemmel,[4] M. Kuessner,[4] A. Kupsc,[64]
M. G. Kurth,[1,52] W. Kühn,[30] J. J. Lane,[55] J. S. Lange,[30] P. Larin,[15] L. Lavezzi,[63c] H. Leithoff,[28] M. Lellmann,[28] T. Lenz,[28]
C. Li,[39] C. H. Li,[33] Cheng Li,[60,48] D. M. Li,[68] F. Li,[1,48] G. Li,[1] H. B. Li,[1,52] H. J. Li,[9,h] J. L. Li,[41] J. Q. Li,[4] Ke Li,[1] L. K. Li,[1]
Lei Li,[3] P. L. Li,[60,48] P. R. Li,[32] S. Y. Li,[50] W. D. Li,[1,52] W. G. Li,[1] X. H. Li,[60,48] X. L. Li,[41] Z. B. Li,[49] Z. Y. Li,[49] H. Liang,[60,48]
H. Liang,[1,52] Y. F. Liang,[45] Y. T. Liang,[25] L. Z. Liao,[1,52] J. Libby,[21] C. X. Lin,[49] B. Liu,[42,g] B. J. Liu,[1] C. X. Liu,[1] D. Liu,[60,48]
D. Y. Liu,[42,g] F. H. Liu,[44] Fang Liu,[1] Feng Liu,[6] H. B. Liu,[13] H. M. Liu,[1,52] Huanhuan Liu,[1] Huihui Liu,[17] J. B. Liu,[60,48]
J. Y. Liu,[1,52] K. Liu,[1] K. Y. Liu,[34] Ke Liu,[6] L. Liu,[60,48] Q. Liu,[52] S. B. Liu,[60,48] Shuai Liu,[46] T. Liu,[1,52] X. Liu,[32] Y. B. Liu,[37]
Z. A. Liu,[1,48,52] Z. Q. Liu,[41] Y. F. Long,[38,k] X. C. Lou,[1,48,52] F. X. Lu,[16] H. J. Lu,[18] J. D. Lu,[1,52] J. G. Lu,[1,48] X. L. Lu,[1] Y. Lu,[1]
Y. P. Lu,[1,48] C. L. Luo,[35] M. X. Luo,[67] P. W. Luo,[49] T. Luo,[9,h] X. L. Luo,[1,48] S. Lusso,[63c] X. R. Lyu,[52] F. C. Ma,[34] H. L. Ma,[1]
L. L. Ma,[41] M. M. Ma,[1,52] Q. M. Ma,[1] R. Q. Ma,[1,52] R. T. Ma,[52] X. N. Ma,[37] X. X. Ma,[1,52] X. Y. Ma,[1,48] Y. M. Ma,[41]
F. E. Maas,[15] M. Maggiora,[63a,63c] S. Maldaner,[28] S. Malde,[58] Q. A. Malik,[62] A. Mangoni,[23b] Y. J. Mao,[38,k] Z. P. Mao,[1]
S. Marcello,[63a,63c] Z. X. Meng,[54] J. G. Messchendorp,[31] G. Mezzadri,[24a] T. J. Min,[36] R. E. Mitchell,[22] X. H. Mo,[1,48,52]
Y. J. Mo,[6] N. Yu. Muchnoi,[10,c] H. Muramatsu,[56] S. Nakhoul,[11,f] Y. Nefedov,[29] F. Nerling,[11,f] I. B. Nikolaev,[10,c] Z. Ning,[1,48]
S. Nisar,[8,i] S. L. Olsen,[52] Q. Ouyang,[1,48,52] S. Pacetti,[23b,23c] X. Pan,[9,h] Y. Pan,[55] A. Pathak,[1] P. Patteri,[23a] M. Pelizaeus,[4]
H. P. Peng,[60,48] K. Peters,[11,f] J. Pettersson,[64] J. L. Ping,[35] R. G. Ping,[1,52] A. Pitka,[4] R. Poling,[56] V. Prasad,[60,48] H. Qi,[60,48]
H. R. Qi,[50] M. Qi,[36] T. Y. Qi,[9] T. Y. Qi,[2] S. Qian,[1,48] W.-B. Qian,[52] Z. Qian,[49] C. F. Qiao,[52] L. Q. Qin,[12] X. P. Qin,[13]
X. S. Qin,[4] Z. H. Qin,[1,48] J. F. Qiu,[1] S. Q. Qu,[37] K. H. Rashid,[62] K. Ravindran,[21] C. F. Redmer,[28] A. Rivetti,[63c] V. Rodin,[31]
M. Rolo,[63c] G. Rong,[1,52] Ch. Rosner,[15] M. Rump,[57] A. Sarantsev,[29,d] Y. Schelhaas,[28] C. Schnier,[4] K. Schoenning,[64]
D. C. Shan,[46] W. Shan,[19] X. Y. Shan,[60,48] M. Shao,[60,48] C. P. Shen,[9] P. X. Shen,[37] X. Y. Shen,[1,52] H. C. Shi,[60,48] R. S. Shi,[1,52]
X. Shi,[1,48] X. D. Shi,[60,48] J. J. Song,[41] Q. Q. Song,[60,48] W. M. Song,[27] Y. X. Song,[38,k] S. Sosio,[63a,63c] S. Spataro,[63a,63c]
F. F. Sui,[41] G. X. Sun,[1] J. F. Sun,[16] L. Sun,[65] S. S. Sun,[1,52] T. Sun,[1,52] W. Y. Sun,[35] Y. J. Sun,[60,48] Y. K. Sun,[60,48] Y. Z. Sun,[1]
Z. T. Sun,[1] Y. H. Tan,[65] Y. X. Tan,[60,48] C. J. Tang,[45] G. Y. Tang,[1] J. Tang,[49] V. Thoren,[64] B. Tsednee,[26] I. Uman,[51d] B. Wang,[1]
B. L. Wang,[52] C. W. Wang,[36] D. Y. Wang,[38,k] H. P. Wang,[1,52] K. Wang,[1,48] L. L. Wang,[1] M. Wang,[41] M. Z. Wang,[38,k]
Meng Wang,[1,52] W. H. Wang,[65] W. P. Wang,[60,48] X. Wang,[38,k] X. F. Wang,[32] X. L. Wang,[9,h] Y. Wang,[49] Y. Wang,[60,48]
Y. D. Wang,[15] Y. F. Wang,[1,48,52] Y. Q. Wang,[1] Z. Wang,[1,48] Z. Y. Wang,[1] Ziyi Wang,[52] Zongyuan Wang,[1,52] D. H. Wei,[12]
P. Weidenkaff,[28] F. Weidner,[57] S. P. Wen,[1] D. J. White,[55] U. Wiedner,[4] G. Wilkinson,[58] M. Wolke,[64] L. Wollenberg,[4]
J. F. Wu,[1,52] L. H. Wu,[1] L. J. Wu,[1,52] X. Wu,[9,h] Z. Wu,[1,48] L. Xia,[60,48] H. Xiao,[9,h] S. Y. Xiao,[1] Y. J. Xiao,[1,52] Z. J. Xiao,[35]
X. H. Xie,[38,k] Y. G. Xie,[1,48] Y. H. Xie,[6] T. Y. Xing,[1,52] X. A. Xiong,[1,52] G. F. Xu,[1] J. J. Xu,[36] Q. J. Xu,[14] W. Xu,[1,52] X. P. Xu,[46]
F. Yan,[9,h] L. Yan,[9,h] L. Yan,[63a,63c] W. B. Yan,[60,48] W. C. Yan,[68] Xu Yan,[46] H. J. Yang,[42,g] H. X. Yang,[1] L. Yang,[65]

R. X. Yang,[60,48] S. L. Yang,[1,52] Y. H. Yang,[36] Y. X. Yang,[12] Yifan Yang,[1,52] Zhi Yang,[25] M. Ye,[1,48] M. H. Ye,[7] J. H. Yin,[1] Z. Y. You,[49] B. X. Yu,[1,48,52] C. X. Yu,[37] G. Yu,[1,52] J. S. Yu,[20,l] T. Yu,[61] C. Z. Yuan,[1,52] W. Yuan,[63a,63c] X. Q. Yuan,[38,k] Y. Yuan,[1] Z. Y. Yuan,[49] C. X. Yue,[33] A. Yuncu,[51b,a] A. A. Zafar,[62] Y. Zeng,[20,l] B. X. Zhang,[1] Guangyi Zhang,[16] H. H. Zhang,[49] H. Y. Zhang,[1,48] J. L. Zhang,[66] J. Q. Zhang,[4] J. W. Zhang,[1,48,52] J. Y. Zhang,[1] J. Z. Zhang,[1,52] Jianyu Zhang,[1,52] Jiawei Zhang,[1,52] L. Zhang,[1] Lei Zhang,[36] S. Zhang,[49] S. F. Zhang,[36] T. J. Zhang,[42,g] X. Y. Zhang,[41] Y. Zhang,[58] Y. H. Zhang,[1,48] Y. T. Zhang,[60,48] Yan Zhang,[60,48] Yao Zhang,[1] Yi Zhang,[9,h] Z. H. Zhang,[6] Z. Y. Zhang,[65] G. Zhao,[1] J. Zhao,[33] J. Y. Zhao,[1,52] J. Z. Zhao,[1,48] Lei Zhao,[60,48] Ling Zhao,[1] M. G. Zhao,[37] Q. Zhao,[1] S. J. Zhao,[68] Y. B. Zhao,[1,48] Y. X. Zhao,[25] Z. G. Zhao,[60,48] A. Zhemchugov,[29,b] B. Zheng,[61] J. P. Zheng,[1,48] Y. Zheng,[38,k] Y. H. Zheng,[52] B. Zhong,[35] C. Zhong,[61] L. P. Zhou,[1,52] Q. Zhou,[1,52] X. Zhou,[65] X. K. Zhou,[52] X. R. Zhou,[60,48] A. N. Zhu,[1,52] J. Zhu,[37] K. Zhu,[1] K. J. Zhu,[1,48,52] S. H. Zhu,[59] W. J. Zhu,[37] X. L. Zhu,[50] Y. C. Zhu,[60,48] Z. A. Zhu,[1,52] B. S. Zou,[1] and J. H. Zou[1]

(BESIII Collaboration)

[1]*Institute of High Energy Physics, Beijing 100049, People's Republic of China*
[2]*Beihang University, Beijing 100191, People's Republic of China*
[3]*Beijing Institute of Petrochemical Technology, Beijing 102617, People's Republic of China*
[4]*Bochum Ruhr-University, D-44780 Bochum, Germany*
[5]*Carnegie Mellon University, Pittsburgh, Pennsylvania 15213, USA*
[6]*Central China Normal University, Wuhan 430079, People's Republic of China*
[7]*China Center of Advanced Science and Technology, Beijing 100190, People's Republic of China*
[8]*COMSATS University Islamabad, Lahore Campus, Defence Road, Off Raiwind Road, 54000 Lahore, Pakistan*
[9]*Fudan University, Shanghai 200443, People's Republic of China*
[10]*G.I. Budker Institute of Nuclear Physics SB RAS (BINP), Novosibirsk 630090, Russia*
[11]*GSI Helmholtzcentre for Heavy Ion Research GmbH, D-64291 Darmstadt, Germany*
[12]*Guangxi Normal University, Guilin 541004, People's Republic of China*
[13]*Guangxi University, Nanning 530004, People's Republic of China*
[14]*Hangzhou Normal University, Hangzhou 310036, People's Republic of China*
[15]*Helmholtz Institute Mainz, Johann-Joachim-Becher-Weg 45, D-55099 Mainz, Germany*
[16]*Henan Normal University, Xinxiang 453007, People's Republic of China*
[17]*Henan University of Science and Technology, Luoyang 471003, People's Republic of China*
[18]*Huangshan College, Huangshan 245000, People's Republic of China*
[19]*Hunan Normal University, Changsha 410081, People's Republic of China*
[20]*Hunan University, Changsha 410082, People's Republic of China*
[21]*Indian Institute of Technology Madras, Chennai 600036, India*
[22]*Indiana University, Bloomington, Indiana 47405, USA*
[23a]*INFN Laboratori Nazionali di Frascati, I-00044, Frascati, Italy*
[23b]*INFN Sezione di Perugia, I-06100, Perugia, Italy*
[23c]*University of Perugia, I-06100, Perugia, Italy*
[24a]*INFN Sezione di Ferrara, I-44122, Ferrara, Italy*
[24b]*University of Ferrara, I-44122, Ferrara, Italy*
[25]*Institute of Modern Physics, Lanzhou 730000, People's Republic of China*
[26]*Institute of Physics and Technology, Peace Avenue 54B, Ulaanbaatar 13330, Mongolia*
[27]*Jilin University, Changchun 130012, People's Republic of China*
[28]*Johannes Gutenberg University of Mainz, Johann-Joachim-Becher-Weg 45, D-55099 Mainz, Germany*
[29]*Joint Institute for Nuclear Research, 141980 Dubna, Moscow Region, Russia*
[30]*Justus-Liebig-Universitaet Giessen, II. Physikalisches Institut, Heinrich-Buff-Ring 16, D-35392 Giessen, Germany*
[31]*KVI-CART, University of Groningen, NL-9747 AA Groningen, The Netherlands*
[32]*Lanzhou University, Lanzhou 730000, People's Republic of China*
[33]*Liaoning Normal University, Dalian 116029, People's Republic of China*
[34]*Liaoning University, Shenyang 110036, People's Republic of China*
[35]*Nanjing Normal University, Nanjing 210023, People's Republic of China*
[36]*Nanjing University, Nanjing 210093, People's Republic of China*
[37]*Nankai University, Tianjin 300071, People's Republic of China*
[38]*Peking University, Beijing 100871, People's Republic of China*
[39]*Qufu Normal University, Qufu 273165, People's Republic of China*
[40]*Shandong Normal University, Jinan 250014, People's Republic of China*
[41]*Shandong University, Jinan 250100, People's Republic of China*
[42]*Shanghai Jiao Tong University, Shanghai 200240, People's Republic of China*

[43]*Shanxi Normal University, Linfen 041004, People's Republic of China*
[44]*Shanxi University, Taiyuan 030006, People's Republic of China*
[45]*Sichuan University, Chengdu 610064, People's Republic of China*
[46]*Soochow University, Suzhou 215006, People's Republic of China*
[47]*Southeast University, Nanjing 211100, People's Republic of China*
[48]*State Key Laboratory of Particle Detection and Electronics, Beijing 100049, Hefei 230026, People's Republic of China*
[49]*Sun Yat-Sen University, Guangzhou 510275, People's Republic of China*
[50]*Tsinghua University, Beijing 100084, People's Republic of China*
[51a]*Ankara University, 06100 Tandogan, Ankara, Turkey*
[51b]*Istanbul Bilgi University, 34060 Eyup, Istanbul, Turkey*
[51c]*Uludag University, 16059 Bursa, Turkey*
[51d]*Near East University, Nicosia, North Cyprus, Mersin 10, Turkey*
[52]*University of Chinese Academy of Sciences, Beijing 100049, People's Republic of China*
[53]*University of Hawaii, Honolulu, Hawaii 96822, USA*
[54]*University of Jinan, Jinan 250022, People's Republic of China*
[55]*University of Manchester, Oxford Road, Manchester, M13 9PL, United Kingdom*
[56]*University of Minnesota, Minneapolis, Minnesota 55455, USA*
[57]*University of Muenster, Wilhelm-Klemm-Strasse 9, 48149 Muenster, Germany*
[58]*University of Oxford, Keble Road, Oxford, OX13RH, United Kingdom*
[59]*University of Science and Technology Liaoning, Anshan 114051, People's Republic of China*
[60]*University of Science and Technology of China, Hefei 230026, People's Republic of China*
[61]*University of South China, Hengyang 421001, People's Republic of China*
[62]*University of the Punjab, Lahore-54590, Pakistan*
[63a]*University of Turin, I-10125, Turin, Italy*
[63b]*University of Eastern Piedmont, I-15121, Alessandria, Italy*
[63c]*INFN, I-10125, Turin, Italy*
[64]*Uppsala University, Box 516, SE-75120 Uppsala, Sweden*
[65]*Wuhan University, Wuhan 430072, People's Republic of China*
[66]*Xinyang Normal University, Xinyang 464000, People's Republic of China*
[67]*Zhejiang University, Hangzhou 310027, People's Republic of China*
[68]*Zhengzhou University, Zhengzhou 450001, People's Republic of China*

Using 2.93 fb^{-1} of e^+e^- collision data taken at a center-of-mass energy of 3.773 GeV with the BESIII detector, we report the first measurements of the absolute branching fractions of 14 hadronic $D^{0(+)}$ decays to exclusive final states with an η, e.g., $D^0 \to K^-\pi^+\eta$, $K_S^0\pi^0\eta$, $K^+K^-\eta$, $K_S^0K_S^0\eta$, $K^-\pi^+\pi^0\eta$, $K_S^0\pi^+\pi^-\eta$, $K_S^0\pi^0\pi^0\eta$, and $\pi^+\pi^-\pi^0\eta$; $D^+ \to K_S^0\pi^+\eta$, $K_S^0K^+\eta$, $K^-\pi^+\pi^+\eta$, $K_S^0\pi^+\pi^0\eta$, $\pi^+\pi^+\pi^-\eta$, and $\pi^+\pi^0\pi^0\eta$. Among these decays, the $D^0 \to K^-\pi^+\eta$ and $D^+ \to K_S^0\pi^+\eta$ decays have the largest branching fractions, which are $\mathcal{B}(D^0 \to K^-\pi^+\eta) = (1.853 \pm 0.025_{\text{stat}} \pm 0.031_{\text{syst}})\%$ and $\mathcal{B}(D^+ \to K_S^0\pi^+\eta) = (1.309 \pm 0.037_{\text{stat}} \pm 0.031_{\text{syst}})\%$, respectively. The charge-parity asymmetries for the six decays with highest event yields are determined, and no statistically significant charge-parity violation is found.

Hadronic D decays provide an ideal platform to explore strong and weak effects in decays of hadrons with charm or bottom quarks. Tests of lepton flavor universality (LFU) with semileptonic B decays are important to explore new physics beyond the standard model (SM). In recent years, the branching fraction (BF) ratios $\mathcal{R}_{\tau/\ell} = \mathcal{B}_{B \to \bar{D}^{(*)}\tau^+\bar{\nu}_\tau}/\mathcal{B}_{B \to \bar{D}^{(*)}\ell^+\bar{\nu}_\ell}$ ($\ell = \mu$, e) measured by *BABAR*, Belle, and LHCb [1–8] were found to deviate from the SM prediction by 3.1σ [9]. It is argued in Ref. [10] that the exclusive hadronic $D^{0(+)}$ decays to η are key potential backgrounds in these tests. However, the known exclusive D^0 and D^+ decays to final states with an η meson only account for 44% and 16% of their corresponding inclusive rates [11], respectively. In particular, the BFs for the decays $D \to \bar{K}\pi\eta$, $K\bar{K}\eta$, $\bar{K}\pi\pi\eta$, and $\pi\pi\pi\eta$ (excluding narrow peaks K_S^0, η, ω, η', and ϕ in individual mass spectra) are poorly known, except for relative measurements of $D^0 \to K^-\pi^+\eta$ [12] and $D^0 \to K_S^0\pi^0\eta$ [13]. Measurements of the BFs of these decays are crucial to address the tensions found in

LFU tests with semileptonic B decays. Furthermore, combining the measured BFs with the corresponding amplitude analysis results gives important information on two-body hadronic D decays. This is essential for improving the understanding of quark U-spin [14–16] and SU(3)-flavor symmetry breaking effects, thereby benefiting theoretical predictions of $D^0\bar{D}^0$ mixing and charge-parity (CP) violation in D decays [16–23].

Studies of CP violation in the weak decays of hadrons are powerful tools for understanding physics within the SM and searches for physics beyond it. The CP violation in D decays is predicted to be up to a few times 10^{-3} [23–29] and has been recently observed to be $(1.54 \pm 0.29) \times 10^{-3}$ in $D^0 \to K^+K^-$ and $\pi^+\pi^-$ decays by LHCb [30]. However, knowledge of CP violation in D decays is still very limited. Searching for CP asymmetries in hadronic D decays, which have been much less explored than (semi-)leptonic decays, allows for a more comprehensive understanding of CP violation in the D sector.

This Letter reports the first measurements of the absolute BFs for the decays $D^0 \to K^-\pi^+\eta$, $K^0_S\pi^0\eta$, $K^+K^-\eta$, $K^0_S K^0_S\eta$, $K^-\pi^+\pi^0\eta$, $K^0_S\pi^+\pi^-\eta$, $K^0_S\pi^0\pi^0\eta$, $\pi^+\pi^-\pi^0\eta$, and $D^+ \to K^0_S\pi^+\eta$, $K^0_S K^+\eta$, $K^-\pi^+\pi^+\eta$, $K^0_S\pi^+\pi^0\eta$, $\pi^+\pi^+\pi^-\eta$, $\pi^+\pi^0\pi^0\eta$. Throughout this Letter, the charge conjugate processes are implied unless stated otherwise. In addition, the CP asymmetries are determined for the six decays with the highest yields. To avoid double-counting previously measured decays, the narrow peaks for the K^0_S, η, ω, η', and ϕ are removed from the mass spectra of the $\pi^{+(0)}\pi^{-(0)}$, $\pi^+\pi^-\pi^0$, $\pi^+\pi^-\pi^0$, $\pi^{+(0)}\pi^{-(0)}\eta$, and K^+K^-(or $\pi^+\pi^-\pi^0$) combinations, respectively.

The data sample was collected with the BESIII detector at a center-of-mass energy $\sqrt{s} = 3.773$ GeV and has an integrated luminosity of 2.93 fb^{-1} [31]. Details about the design and performance of the BESIII detector are given in Ref. [32]. The Monte Carlo (MC) simulated events are produced with a GEANT4-based [33] detector simulation software package. An inclusive MC sample, including $D^0\bar{D}^0$, D^+D^- and non-$D\bar{D}$ decays of the $\psi(3770)$, initial state radiation production of the $\psi(3686)$ and J/ψ, and the processes $e^+e^- \to q\bar{q}$ ($q = u, d, s$) and $e^+e^- \to (\gamma)\ell^+\ell^-$ ($\ell = e, \mu, \tau$), is produced to determine the detection efficiencies and to estimate any potential backgrounds. The production of the charmonium states is simulated by the MC generator KKMC [34]. The measured decay modes of the charmonium states are generated using EVTGEN [35] with BFs from the Particle Data Group [11], and the remaining unknown decay modes are generated by LUNDCHARM [36].

The BFs of the hadronic D (D^0 or D^+) decays are measured via the reaction chain $e^+e^- \to \psi(3770) \to D\bar{D}$. If a $\bar{D}$ meson is fully reconstructed, it is called a single-tag (ST) $\bar{D}$ meson. The ST D^- mesons are reconstructed via the decays $D^- \to K^+\pi^-\pi^-$, $K^0_S\pi^-$, $K^+\pi^-\pi^-\pi^0$, $K^0_S\pi^-\pi^0$, $K^0_S\pi^+\pi^-\pi^-$, and $K^+K^-\pi^-$, while the ST $\bar{D}^0$ mesons are

reconstructed using the decays $\bar{D}^0 \to K^+\pi^-$, $K^+\pi^-\pi^0$, and $K^+\pi^-\pi^-\pi^+$. If a signal decay is fully reconstructed in the system recoiling against an ST $\bar{D}$ meson, the candidate event is called a double-tag (DT) event. The BF of the signal decay is given by

$$\mathcal{B}_{\text{sig}} = N_{\text{DT}}/(N_{\text{ST}} \cdot \epsilon_{\text{sig}}), \qquad (1)$$

where $N_{\text{ST}} = \sum_i N^i_{\text{ST}}$ and N_{DT} are the total ST and DT yields in data, respectively, and $\epsilon_{\text{sig}} = \sum_i (N^i_{\text{ST}} \cdot \epsilon^i_{\text{DT}}/\epsilon^i_{\text{ST}})/N_{\text{ST}}$ is the effective efficiency for detecting the signal decay, averaged over tag mode i, where ϵ_{ST} and ϵ_{DT} are the efficiencies for detecting ST and DT candidates, respectively.

We use the same selection criteria for $K^\pm$, $\pi^\pm$, K^0_S, γ, and π^0 as were used in Refs. [37–43]. Candidates for η are reconstructed from $\gamma\gamma$ pairs with invariant mass within $(0.515, 0.570)$ GeV/c^2. To improve resolution, a one-constraint kinematic fit is imposed on each $\gamma\gamma$ pair to constrain their invariant mass at η nominal mass [11]. For $\bar{D}^0 \to K^+\pi^-\pi^-\pi^+$ tags, the $\bar{D}^0 \to K^0_S K^\pm\pi^\mp$ decays are rejected if the mass of any $\pi^+\pi^-$ pair falls in the range $(0.478, 0.518)$ GeV/c^2.

Tagging $\bar{D}$ (signal D) mesons are identified by two variables, the energy difference $\Delta E_{\text{tag (sig)}} \equiv E_{\text{tag (sig)}} - E_b$ and the beam-constrained mass $M^{\text{tag (sig)}}_{\text{BC}} \equiv \sqrt{E_b^2 - |\vec{p}_{\text{tag (sig)}}|^2}$, where tag (sig) represents the tagging $\bar{D}$ (signal D), E_b the beam energy, and $\vec{p}_{\text{tag (sig)}}$ and $E_{\text{tag (sig)}}$ the momentum and energy of the $\bar{D}(D)$ candidate in the e^+e^- rest frame. For each tag (signal) mode, if there are multiple combinations, only the one with the minimum $|\Delta E_{\text{tag (sig)}}|$ is kept for further analysis. The $\bar{D}$ tags are required to satisfy $\Delta E_{\text{tag}} \in (-55, 40)$ MeV for the modes containing π^0 in the final states and $\Delta E_{\text{tag}} \in (-25, 25)$ MeV for the other modes. The yields of ST $\bar{D}$ mesons are obtained from binned maximum likelihood fits to the $M^{\text{tag}}_{\text{BC}}$ distributions of the accepted ST candidates following Refs. [37–41]. The total ST D^- yield is $N_{\text{ST}D^-} = 1558159 \pm 2113_{\text{stat}}$. The total ST $\bar{D}^0$ yield is $N_{\text{ST}\bar{D}^0} = 2327839 \pm 1860_{\text{stat}}$ for self-conjugate signal D^0 decays. For the flavor specific signal decays $D^0 \to K^-\pi^+\eta$ and $K^-\pi^+\pi^0\eta$, we remove doubly Cabibbo suppressed decays from the ST selection, giving $N_{\text{ST}\bar{D}^0} = 2\,321\,430 \pm 1860_{\text{stat}}$ for these decays.

For the signal D decays recoiling against the $\bar{D}$ tags, tracks are selected from the residual tracks that have not been used for the tag reconstruction. The signal D decays are selected by using the ΔE_{sig} requirements as listed in Table I. For the $\pi^+\pi^-[\pi^0\pi^0]$, $\pi^+\pi^-\pi^0$, $\pi^+\pi^-\pi^0$, $\pi^{+(0)}\pi^{-(0)}\eta$, and K^+K^- combinations, the K^0_S, η, ω, η', and ϕ contributions are rejected by requiring their invariant masses to be outside $(0.468, 0.528)$ GeV/c^2 $[(0.438, 0.538)$ GeV/$c^2]$, $(0.498, 0.578)$ GeV/c^2, $(0.732, 0.832)$ GeV/c^2, $(0.908, 1.008)$ GeV/c^2, and $(0.990, 1.390)$ GeV/c^2, respectively.

TABLE I. Requirements on ΔE_{sig}, net DT yields in data (N_{DT}), detection efficiencies (ϵ_{sig}, including the BFs of K_S^0, η, and π^0 as well as correction factors described later), and the obtained BFs ($\mathcal{B}_{\text{sig}}$). Numbers in the first and second brackets are last two effective digits of statistical and systematic uncertainties, respectively, for $\mathcal{B}_{\text{sig}}$. The uncertainty is statistical only for N_{DT}. The efficiency of $D^0 \to K^+K^-\eta$ is significantly lower than that of $D^0 \to K^-\pi^+\eta$ because of lower selection efficiencies of K^-, K^+, and η due to smaller PHSP as well as ϕ veto in K^+K^- mass spectrum.

Decay	ΔE_{sig} (MeV)	N_{DT}	ϵ_{sig} (%)	$\mathcal{B}_{\text{sig}}$ ($\times 10^{-4}$)
$D^0 \to K^-\pi^+\eta$	$(-37, 36)$	6116.2 ± 81.8	14.22	$185.3(25)(31)$
$D^0 \to K_S^0\pi^0\eta$	$(-57, 45)$	1092.7 ± 35.2	4.66	$100.6(34)(30)$
$D^0 \to K^+K^-\eta$	$(-27, 27)$	13.1 ± 4.0	9.53	$0.59(18)(05)$
$D^0 \to K_S^0K_S^0\eta$	$(-29, 28)$	7.3 ± 3.2	2.36	$1.33(59)(18)$
$D^0 \to K^-\pi^+\pi^0\eta$	$(-44, 36)$	576.5 ± 28.8	5.53	$44.9(22)(15)$
$D^0 \to K_S^0\pi^+\pi^-\eta$	$(-33, 32)$	248.2 ± 18.0	3.80	$28.0(19)(10)$
$D^0 \to K_S^0\pi^0\pi^0\eta$	$(-56, 41)$	64.7 ± 9.2	1.58	$17.6(23)(13)$
$D^0 \to \pi^+\pi^-\pi^0\eta$	$(-57, 45)$	508.6 ± 26.0	6.76	$32.3(17)(14)$
$D^+ \to K_S^0\pi^+\eta$	$(-36, 36)$	1328.2 ± 37.8	6.51	$130.9(37)(31)$
$D^+ \to K_S^0K^+\eta$	$(-27, 27)$	13.6 ± 3.9	4.72	$1.85(52)(08)$
$D^+ \to K^-\pi^+\pi^+\eta$	$(-33, 33)$	188.0 ± 15.3	8.94	$13.5(11)(04)$
$D^+ \to K_S^0\pi^+\pi^0\eta$	$(-49, 41)$	48.7 ± 9.7	2.57	$12.2(24)(06)$
$D^+ \to \pi^+\pi^+\pi^-\eta$	$(-40, 38)$	514.6 ± 25.7	9.67	$34.1(17)(10)$
$D^+ \to \pi^+\pi^0\pi^0\eta$	$(-70, 49)$	192.5 ± 17.1	3.86	$32.0(28)(17)$

These correspond to at least five times the fitted mass resolution away from individual nominal mass. For $D^0 \to K_S^0\pi^{+(0)}\pi^{-(0)}\eta$ [$\pi^+\pi^-\pi^0\eta$] decays, no aforementioned mass requirements of the $K_S^0[\phi]$ are imposed on the $\pi^{+(0)}\pi^{-(0)}$ [$\pi^+\pi^-\pi^0$] combinations, due to the small BFs and the limited phase space (PHSP) of the background channels $D^0 \to K_S^0K_S^0\eta$ [$\phi\eta$]. The opening angle between signal D and tagging $\bar{D}$ is required to be greater than $160°$, with a loss of $(2\text{–}6)\%$ of the signal, to suppress misformed $D\bar{D}$ candidates. For $D \to \bar{K}\pi\pi^0\eta$, the peaking backgrounds (PBKG) of $D \to \bar{K}\pi\pi^0\pi^0$ are rejected if any $\bar{K}\pi\pi^0\pi^0$ combinations satisfying $\Delta E_{\bar{K}\pi\pi^0\pi^0} \in (-0.05, 0.05)$ GeV and $M_{\text{BC}}^{\bar{K}\pi\pi^0\pi^0} \in (1.83, 1.89)$ GeV$/c^2$ can be found in the same candidate events. The combination of these requirements rejects more than 75% of the background and keeps $(93\text{–}97)\%$ of the signal.

To determine the DT yields in the data ($N_{\text{DT}}^{\text{fit}}$), a two-dimensional (2D) unbinned maximum likelihood fit is performed on the $M_{\text{BC}}^{\text{tag}}$ vs $M_{\text{BC}}^{\text{sig}}$ distribution of the accepted DT candidates (see Fig. 1 of the Supplemental Material [44] for an example). Signal events concentrate around $M_{\text{BC}}^{\text{tag}} = M_{\text{BC}}^{\text{sig}} = M_D$, where M_D is the nominal D mass [11]. Background events are divided into three categories. The first one (named BKGI) is from events with correctly reconstructed D ($\bar{D}$) and incorrectly reconstructed $\bar{D}$ (D). They are spread along the lines around $M_{\text{BC}}^{\text{tag}}$ or $M_{\text{BC}}^{\text{sig}} = M_D$. The second one (named BKGII) is from events smeared along the diagonal, which are mainly from the $e^+e^- \to q\bar{q}$ processes. The third one (named BKGIII) comes from events with uncorrelated and incorrectly reconstructed D and $\bar{D}$.

In the 2D fit, the probability density functions (PDFs) of the backgrounds are constructed as (i) BKGI: $b(x) \cdot c_y(y; E_b, \xi_y, \frac{1}{2}) + b(y) \cdot c_x(x; E_b, \xi_x, \frac{1}{2})$, (ii) BKGII:

$c_z(z; \sqrt{2}E_b, \xi_z, \frac{1}{2}) \cdot g(k; 0, \sigma_k)$, and (iii) BKGIII: $c_x(x; E_b, \xi_x, \frac{1}{2}) \cdot c_y(y; E_b, \xi_y, \frac{1}{2})$. Here, $x = M_{\text{BC}}^{\text{sig}}$, $y = M_{\text{BC}}^{\text{tag}}$, $z = (x + y)/\sqrt{2}$, and $k = (x - y)/\sqrt{2}$. The PDFs for signal, $a(x, y)$, $b(x)$, and $b(y)$, are described by the corresponding MC-simulated shapes. $c_f(f; E_b, \xi_f, \frac{1}{2})$ is an ARGUS function [45] defined as $A_f \cdot f \cdot [1 - (f^2/E_b^2)]^{1/2} \cdot e^{\xi_f(1-f^2/E_b^2)}$, where f denotes x, y, or z; E_b is fixed at 1.8865 GeV$/c^2$; A_f is a normalization factor; and ξ_f is a fit parameter. $g(k; 0, \sigma_k)$ is a Gaussian function with mean of zero and standard deviation $\sigma_k = \sigma_0 \cdot (\sqrt{2}E_b - z)^p$, where σ_0 and p are two free parameters. In addition to these backgrounds, for the decays $D^0 \to K_S^0\pi^{+(0)}\pi^{-(0)}\eta$, $\pi^+\pi^-\pi^0\eta$, $K^-\pi^+\pi^0\eta$, $K_S^0\pi^0\pi^0\eta$, and $D^+ \to K_S^0\pi^+\pi^0\eta$, the yields and shapes of the PBKG components are fixed based on MC simulations. All other parameters are left free.

Combinatorial $\pi^+\pi^-$ pairs can also satisfy the K_S^0 selection criteria and form peaking backgrounds around the D mass in the $M_{\text{BC}}^{\text{sig}}$ distribution. This kind of peaking background is estimated by the data events in the K_S^0 sideband region. For $D^0 \to K_S^0\pi^0\eta$, $K_S^0\pi^+\pi^-\eta$, $K_S^0\pi^0\pi^0\eta$, and $D^+ \to K_S^0\pi^+\eta$, $K_S^0K^+\eta$, $K_S^0\pi^+\pi^0\eta$, one-dimensional (1D) signal and sideband regions are defined as $M_{\pi^+\pi^-} \in (0.486, 0.510)$ GeV$/c^2$ and $M_{\pi^+\pi^-} \in (0.454, 0.478) \cup (0.518, 0.542)$ GeV$/c^2$, respectively. For $D^0 \to K_S^0K_S^0\eta$, 2D signal and sideband regions are defined. The 2D sideband 1 (2) regions are defined as the boxes in which one (two) of the two $\pi^+\pi^-$ combinations lie in the K_S^0 sideband regions and the rest are located in the K_S^0 signal regions. See Fig. 2 of the Supplemental Material [44] as an example.

For the decays involving K_S^0, the net DT yields are obtained by $N_{\rm DT} = N_{\rm DT}^{\rm fit} - \frac{1}{2}(N_{\rm sid\text{-}1}^{\rm fit} - N_{\rm sid\text{-}2}^{\rm fit}) - \frac{1}{4}N_{\rm sid\text{-}2}^{\rm fit} = N_{\rm DT}^{\rm fit} - \frac{1}{2}N_{\rm sid\text{-}1}^{\rm fit} + \frac{1}{4}N_{\rm sid\text{-}2}^{\rm fit}$, where $N_{\rm DT}^{\rm fit}$ and $N_{\rm sid\text{-}i}^{\rm fit}$ are the fitted DT yields in the K_S^0 signal region and sideband i region, respectively. This relation has been verified based on MC simulation. For the other decays, the net DT yields are $N_{\rm DT}^{\rm fit}$.

For each signal decay mode, the statistical significance is calculated by $\sqrt{-2\ln(\mathcal{L}_0/\mathcal{L}_{\rm max})}$, where $\mathcal{L}_{\rm max}$ and $\mathcal{L}_0$ are the maximum likelihoods with and without the signal component in the fits, respectively. The effect of combinatorial $\pi^+\pi^-$ backgrounds in the K_S^0 signal regions has been considered for the decays involving K_S^0. The statistical significances of the four decays with lowest yields, $D^0 \to K^+K^-\eta$, $K_S^0K_S^0\eta$, $D^+ \to K_S^0K^+\eta$, and $K_S^0\pi^+\pi^0\eta$, are 5.5σ, 2.8σ, 5.7σ, and 8.4σ, respectively; those for the other decays are all greater than 10σ.

To determine the signal efficiencies ($\epsilon_{\rm sig}$), the $D \to \bar{K}\pi\eta$ decays are simulated with a modified data-driven generator BODY3 [35], which was developed to simulate different intermediate states in data for a given three-body final state. The Dalitz plot of $M_{\bar{K}\pi}^2$ vs $M_{\pi\eta}^2$ found in data, corrected for backgrounds and efficiencies, is taken as input for the BODY3 generator. The efficiencies across the kinematic space are obtained with MC samples generated with the PHSP generator. Intermediate states in the $D^0 \to K^+K^-\eta$, $K_S^0K_S^0\eta$, $K_S^0\pi^0\pi^0\eta$, and $D^+ \to K_S^0K^+\eta$, $K_S^0\pi^+\pi^0\eta$ decays cannot be determined due to limited statistics; these decays are therefore simulated with the PHSP generator. Each of the other decays is simulated with a mixed signal MC sample. Here, the decays generated with PHSP generator and the decays containing $K^*(892)$, $\rho(770)$, and $a_0(980)$ intermediate states are mixed with fractions obtained by examining the corresponding invariant mass spectra. The

data distributions for momenta and $\cos\theta$ (where θ is the polar angle in the e^+e^- rest frame) of the daughter particles, and the invariant masses of each of the two- and three-body particle combinations, agree with the MC simulations. The differences between the DT efficiencies obtained with the BODY3 and PHSP generators will be assigned as a systematic uncertainty.

The values for $N_{\rm DT}$, $\epsilon_{\rm sig}$, and the BFs of the signal decays are summarized in Table I. The BF upper limit for $D^0 \to K_S^0K_S^0\eta$ at 90% confidence level is determined to be $< 2.4 \times 10^{-4}$ using the Bayesian approach after incorporating the systematic uncertainty [46].

The systematic uncertainties arise from the sources discussed below and are estimated relative to the measured BFs. The uncertainties in the total ST yields come from the $M_{\rm BC}^{\rm tag}$ fits to the ST $\bar{D}$ candidates, which were determined as 0.5% for both neutral and charged $\bar{D}$ [37–39]. The systematic uncertainties of the tracking efficiencies are found to be (0.2–0.5)% per $K^\pm$ or $\pi^\pm$, while those for PID efficiencies are taken as (0.2–0.3)% per $K^\pm$ or $\pi^\pm$, by using DT $D\bar{D}$ hadronic events. The systematic uncertainty in K_S^0 reconstruction is estimated to be 1.6% per K_S^0 by using the $J/\psi \to K^*(892)^{\mp}K^\pm$ and $J/\psi \to \phi K_S^0 K^\pm \pi^\mp$ candidates [47]. The systematic uncertainty of the π^0 reconstruction is assigned as (0.7–0.8)% per π^0 from studies of DT $D\bar{D}$ hadronic decay samples of $D^0 \to K^-\pi^+$, $K^-\pi^+\pi^+\pi^-$ vs $\bar{D}^0 \to K^+\pi^-\pi^0$, $K_S^0\pi^0$ [37,38]. The systematic uncertainty for η reconstruction is taken to be the same as that for π^0. The uncertainties of the quoted BFs of $K_S^0 \to \pi^+\pi^-$, $\eta \to \gamma\gamma$, and $\pi^0 \to \gamma\gamma$ decays are 0.07%, 0.5%, and 0.03% [11], respectively.

To estimate the systematic uncertainty in 2D fit, we repeat the fits by varying the signal shape, the endpoint of the ARGUS function (± 0.2 MeV/c^2), the fixed PBKG
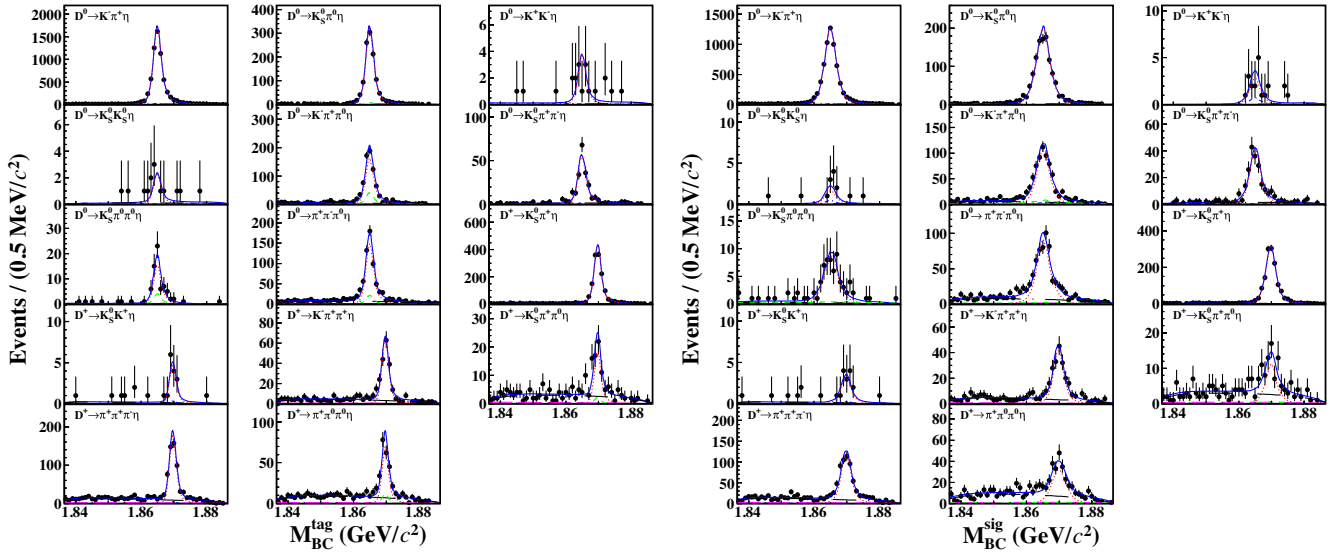

FIG. 1. Projections on $M_{\rm BC}^{\rm tag}$ and $M_{\rm BC}^{\rm sig}$ of the 2D fits to the DT candidate events. Data are shown as dots with error bars. Blue solid, red dotted, blue dot-dashed, black dot-long-dashed, green long-dashed, and pink dashed curves denote the overall fit results, signal, BKGI, BKGII, BKGIII, and PBKG components (see text), respectively.

yield ($\pm 1\sigma$ of the quoted BF). The systematic uncertainty of the $D\bar{D}$ opening angle requirement is assigned as 0.4% by using the DT events of $D^0 \to K^-\pi^+\pi^0$. The systematic uncertainty due to the $\Delta E_{\rm sig}$ requirement is assigned to be 0.3%, which is the largest efficiency difference with and without smearing the data-MC Gaussian resolution of $\Delta E_{\rm sig}$ for signal MC events. Here, the parameters of the Gaussian are obtained by using the DT samples of $D^0 \to K_S^0\pi^0$, $K^-\pi^+\pi^0$, $K^-\pi^+\pi^0\pi^0$, and $D^+ \to K^-\pi^+\pi^+\pi^0$. The systematic uncertainties due to the choice of the K_S^0 sideband and the $K_S^0/\omega/\eta^{(\prime)}/\phi$ rejection windows are assigned by examining the changes of the BFs when varying the nominal K_S^0 sideband and rejection windows by ± 5 MeV/c^2. The uncertainties due to limited MC statistics (0.3–1.1)% are considered as a source of systematic uncertainty.

The systematic uncertainties in MC modeling are categorized into three cases. For the $D \to \bar{K}\pi\eta$ decays, the differences between the DT efficiencies obtained with the BODY3 and PHSP generators are assigned as the uncertainties. For the decays whose efficiencies are estimated with the PHSP generator, the uncertainties are assigned by referring to the largest change of the efficiencies among $D^0 \to K^-\pi^+\eta$, $K_S^0\pi^0\eta$, and $D^+ \to K_S^0\pi^+\eta$. For the decays whose efficiencies are estimated with the mixed signal MC events, the systematic uncertainties are assigned as the change of the DT efficiency after removing the smallest component.

The $D^0\bar{D}^0$ pairs are produced coherently at the $\psi(3770)$. For the decays $D^0 \to K_S^0\pi^0\eta$, $K^+K^-\eta$, $K_S^0K_S^0\eta$, $K_S^0\pi^+\pi^-\eta$, $K_S^0\pi^0\pi^0\eta$, and $\pi^+\pi^-\pi^0\eta$, the measured BFs are affected by various CP components due to quantum-correlation (QC) effects. The fractions of $CP+$ components in these decays are examined by the $CP+$ tag of $D^0 \to K^+K^-$ and $CP-$ tag of $D^0 \to K_S^0\pi^0$, with the same method described in Ref. [48], and the necessary parameters are taken from Refs. [49–51]. The obtained impact of QC effects on the BFs ($f_{\rm QC}$) is shown in Table I of the Supplemental Material [44]. The signal efficiencies are corrected by the corresponding $f_{\rm QC}$ factors; residual statistical errors of $f_{\rm QC}$ are assigned as the systematic uncertainties.

For each signal decay, the total systematic uncertainty is obtained by adding the above effects in quadrature. The systematic uncertainties for the various signal decays are given in Table II of the Supplemental Material [44] and the individual absolute systematic errors are summarized in Table I of text.

For the six decay modes with the highest yields, the BFs of D and $\bar{D}$ decays, $\mathcal{B}_{\rm sig}^+$ and $\mathcal{B}_{\overline{\rm sig}}^-$, are measured separately. Their asymmetry is determined by $\mathcal{A}_{CP}^{\rm sig} = (\mathcal{B}_{\rm sig}^+ - \mathcal{B}_{\overline{\rm sig}}^-)/(\mathcal{B}_{\rm sig}^+ + \mathcal{B}_{\overline{\rm sig}}^-)$. The obtained BFs and asymmetries are summarized in Table II. We find no statistically significant CP violation. Several systematic uncertainties cancel in the asymmetry: the tracking and PID of $\pi^+\pi^-/K^+K^-$ pair, K_S^0

TABLE II. Charge-conjugated BFs ($\mathcal{B}_{\rm sig}^+$ and $\mathcal{B}_{\overline{\rm sig}}^-$), and their asymmetries ($\mathcal{A}_{CP}^{\rm sig}$). The first and second uncertainties are statistical and systematic, respectively, for $\mathcal{A}_{CP}^{\rm sig}$; uncertainties for $\mathcal{B}_{\rm sig}^+$ and $\mathcal{B}_{\overline{\rm sig}}^-$ are only statistical.

Decay	$\mathcal{B}_{\rm sig}^+$ ($\times 10^{-4}$)	$\mathcal{B}_{\overline{\rm sig}}^-$ ($\times 10^{-4}$)	$\mathcal{A}_{CP}^{\rm sig}$ (%)
$D^0 \to K^-\pi^+\eta$	182.1 ± 3.5	189.1 ± 3.6	$-1.9 \pm 1.3 \pm 1.0$
$D^0 \to K_S^0\pi^0\eta$	98.4 ± 4.8	106.3 ± 5.1	$-3.9 \pm 3.2 \pm 0.8$
$D^0 \to K^-\pi^+\pi^0\eta$	41.7 ± 2.7	48.8 ± 3.2	$-7.9 \pm 4.8 \pm 2.5$
$D^0 \to \pi^+\pi^-\pi^0\eta$	29.8 ± 2.2	33.3 ± 2.5	$-5.5 \pm 5.2 \pm 2.4$
$D^+ \to K_S^0\pi^+\eta$	129.9 ± 5.3	132.3 ± 5.4	$-0.9 \pm 2.9 \pm 1.0$
$D^+ \to \pi^+\pi^+\pi^-\eta$	35.4 ± 2.4	33.7 ± 2.4	$+2.5 \pm 5.0 \pm 1.6$

reconstruction, π^0/η reconstruction, quoted BFs, K_S^0 sideband choice, $K_S^0/\omega/\eta^{(\prime)}/\phi$ rejection windows, MC modeling, and strong phase of D^0 decays. The other systematic uncertainties are estimated separately as above.

In summary, with 2.93 fb^{-1} of data taken at $\sqrt{s} = 3.773$ GeV with the BESIII detector, we report the first measurements of the absolute BFs of 14 exclusive $D^{0(+)}$ decays to η. Summing over the BFs measured in this work, and using the world averaged values of other known decays [11], the total BFs of all the exclusive D^0 and D^+ decays to η are determined to be $(8.62 \pm 0.35)\%$ and $(4.68 \pm 0.18)\%$, respectively. Here, the systematic uncertainties of $N_{\rm ST}$, $K^\pm/\pi^\pm$ tracking and PID, K_S^0 and η reconstruction, and the quoted BFs are correlated. They are consistent with the corresponding inclusive rates $(9.5 \pm 0.9)\%$ and $(6.5 \pm 0.7)\%$ within 0.9σ and 2.5σ, respectively, leaving little room for other exclusive decays involving η. The reported BFs provide key inputs for accurate background estimations in LFU tests with semileptonic B decays, which are crucial to explore possible new physics beyond the SM. The obtained $\mathcal{B}(D^0 \to K^-\pi^+\eta)$ agrees with the recent Belle result [11,12] within 1.3σ, with precision improved twofold. Our $\mathcal{B}(D^0 \to K_S^0\pi^0\eta)$ is greater than CLEO's result [11,13] by 3.7σ. Combining the measured $\mathcal{B}(D^0 \to K_S^0\pi^0\eta)$ with the fit fraction $\mathcal{B}(D^0 \to \bar{K}^*(892)^0\eta, \bar{K}^*(892)^0 \to K_S^0\pi^0)/\mathcal{B}(D^0 \to K_S^0\pi^0\eta)$ from CLEO [13], we find $\mathcal{B}(D^0 \to \bar{K}^*(892)^0\eta) = (1.77 \pm 0.44)\%$, where the uncertainty is dominated by the fit fraction. This deviates from various theoretical calculations [18,19,23] by 1.9–2.9σ. Future amplitude analyses of these decays at BESIII [52] and Belle II [53] will open a window to extract more two-body hadronic D decays, which are important to understand quark U-spin and SU(3)-flavor symmetry breaking effects and will be beneficial for the predictions of $D^0\bar{D}^0$ mixing and CP violation in D decays [18,19,23]. In addition, we determine the asymmetries of the charge-conjugated BFs for the six D decays with highest yields, and we find no statistically significant CP violation.

---

[a]Also at Bogazici University, 34342 Istanbul, Turkey.

[b]Also at Moscow Institute of Physics and Technology, Moscow 141700, Russia.

[c]Also at Novosibirsk State University, Novosibirsk, 630090, Russia.

[d]Also at NRC "Kurchatov Institute," PNPI, 188300, Gatchina, Russia.

[e]Also at Istanbul Arel University, 34295 Istanbul, Turkey.

[f]Also at Goethe University Frankfurt, 60323 Frankfurt am Main, Germany.

[g]Also at Key Laboratory for Particle Physics, Astrophysics and Cosmology, Ministry of Education; Shanghai Key Laboratory for Particle Physics and Cosmology; Institute of Nuclear and Particle Physics, Shanghai 200240, People's Republic of China.

[h]Also at Key Laboratory of Nuclear Physics and Ion-beam Application (MOE) and Institute of Modern Physics, Fudan University, Shanghai 200443, People's Republic of China.

[i]Also at Harvard University, Department of Physics, Cambridge, Massachusetts 02138, USA.

[j]Present address: Institute of Physics and Technology, Peace Ave.54B, Ulaanbaatar 13330, Mongolia.

[k]Also at State Key Laboratory of Nuclear Physics and Technology, Peking University, Beijing 100871, People's Republic of China.

[l]School of Physics and Electronics, Hunan University, Changsha 410082, China.

[1] J. P. Lees *et al.* (*BABAR* Collaboration), Phys. Rev. Lett. **109**, 101802 (2012).

[2] J. P. Lees *et al.* (*BABAR* Collaboration), Phys. Rev. D **88**, 072012 (2013).

[3] R. Aaij *et al.* (LHCb Collaboration), Phys. Rev. Lett. **115**, 111803 (2015).

[4] M. Huschle *et al.* (Belle Collaboration), Phys. Rev. D **92**, 072014 (2015).

[5] Y. Sato *et al.* (Belle Collaboration), Phys. Rev. D **94**, 072007 (2016).

[6] R. Aaij *et al.* (LHCb Collaboration), Phys. Rev. D **97**, 072013 (2018).

[7] A. Abdesselam *et al.* (Belle Collaboration), arXiv:1904.08794.

[8] G. Garia *et al.* (Belle Collaboration), Phys. Rev. Lett. **124**, 161803 (2020).

[9] Y. Amhis *et al.* (Heavy Flavor Averaging Group), arXiv:1909.12524.

[10] R. Aaij *et al.* (LHCb Collaboration), Synergy of BESIII and LHCb physics programmes, Report No. LHCb-PUB-2016-025.

[11] M. Tanabashi *et al.* (Particle Data Group), Phys. Rev. D **98**, 030001 (2018); and 2019 update.

[12] Y. Q. Chen *et al.* (Belle Collaboration), arXiv:2003.07759.

[13] P. Rubin *et al.* (CLEO Collaboration), Phys. Rev. Lett. **93**, 111801 (2004).

[14] R. L. Kingsley, S. B. Treiman, F. Wilczek, and A. Zee, Phys. Rev. D **11**, 1919 (1975).

[15] M. Gronau, Phys. Lett. B **730**, 221 (2014); **735**, 282(E) (2014).

[16] Z. Z. Xing, Mod. Phys. Lett. A **34**, 1950238 (2019).

[17] H. J. Lipkin, Phys. Rev. Lett. **46**, 1307 (1981).

[18] H. Y. Cheng and C. W. Chiang, Phys. Rev. D **81**, 074021 (2010).

[19] Q. Qin, H. N. Li, C. D. Lü, and F. S. Yu, Phys. Rev. D **89**, 054006 (2014).

[20] H. Y. Cheng, C. W. Chiang, and A. L. Kuo, Phys. Rev. D **93**, 114010 (2016).

[21] W. Kwong and S. P. Rosen, Phys. Lett. B **298**, 413 (1993).

[22] Y. Grossman and D. J. Robinson, J. High Energy Phys. 04 (2013) 067.

[23] H. N. Li, C. D. Lü, and F. S. Yu, Phys. Rev. D **86**, 036012 (2012).

[24] I. I. Bigi, A. Paul, and S. Recksiegel, J. High Energy Phys. 06 (2011) 089.

[25] G. Isidori, J. F. Kamenik, Z. Ligeti, and G. Perez, Phys. Lett. B **711**, 46 (2012).

[26] J. Brod, A. L. Kagan, and J. Zupan, Phys. Rev. D **86**, 014023 (2012).

[27] H. Y. Cheng and C. W. Chiang, Phys. Rev. D **86**, 014014 (2012).

[28] H. Y. Cheng and C. W. Chiang, Phys. Rev. D **100**, 093002 (2019).

[29] H. N. Li, C. D. Lü, and F. S. Yu, arXiv:1903.10638.

[30] R. Aaij *et al.* (LHCb Collaboration), Phys. Rev. Lett. **122**, 211803 (2019).

[31] M. Ablikim *et al.* (BESIII Collaboration), Chin. Phys. C **37**, 123001 (2013); Phys. Lett. B **753**, 629 (2016).

[32] M. Ablikim *et al.* (BESIII Collaboration), Nucl. Instrum. Methods Phys. Res., Sect. A **614**, 345 (2010).

[33] S. Agostinelli *et al.* (GEANT4 Collaboration), Nucl. Instrum. Methods Phys. Res., Sect. A **506**, 250 (2003).

[34] S. Jadach, B. F. L. Ward, and Z. Was, Phys. Rev. D **63**, 113009 (2001); Comput. Phys. Commun. **130**, 260 (2000).

[35] D. J. Lange, Nucl. Instrum. Methods Phys. Res., Sect. A **462**, 152 (2001); R. G. Ping, Chin. Phys. C **32**, 599 (2008).

[36] J. C. Chen, G. S. Huang, X. R. Qi, D. H. Zhang, and Y. S. Zhu, Phys. Rev. D **62**, 034003 (2000).

[37] M. Ablikim *et al.* (BESIII Collaboration), Eur. Phys. J. C **76**, 369 (2016).

[38] M. Ablikim *et al.* (BESIII Collaboration), Chin. Phys. C **40**, 113001 (2016).

[39] M. Ablikim *et al.* (BESIII Collaboration), Phys. Rev. Lett. **121**, 171803 (2018).

[40] M. Ablikim *et al.* (BESIII Collaboration), Phys. Rev. Lett. **123**, 231801 (2019).

[41] M. Ablikim *et al.* (BESIII Collaboration), Phys. Rev. D **101**, 052009 (2020).

[42] M. Ablikim *et al.* (BESIII Collaboration), Phys. Rev. D **101**, 072005 (2020).

[43] M. Ablikim *et al.* (BESIII Collaboration), Phys. Rev. Lett. **124**, 231801 (2020).

[44] See Supplemental Material at http://link.aps.org/supplemental/10.1103/PhysRevLett.124.241803 for an illustration of the $M_{\mathrm{BC}}^{\mathrm{tag}}$ vs $M_{\mathrm{BC}}^{\mathrm{sig}}$ distribution, the definitions of 1D and 2D signal and sideband regions of K_S^0, the correction factors due to QC effects, and the systematic uncertainties of various sources in the BF measurements.

[45] H. Albrecht *et al.* (ARGUS Collaboration), Phys. Lett. B **241**, 278 (1990).

[46] K. Stenson, arXiv:physics/0605236.

[47] M. Ablikim *et al.* (BESIII Collaboration), Phys. Rev. D **92**, 112008 (2015).

[48] M. Ablikim *et al.* (BESIII Collaboration), Phys. Rev. D **100**, 072006 (2019).

[49] T. Gershon, J. Libby, and G. Wilkinson, Phys. Lett. B **750**, 338 (2015).

[50] T. Evans, S. T. Harnew, J. Libby, S. Malde, J. Rademacker, and G. Wilkinson, Phys. Lett. B **757**, 520 (2016); **765**, 402(E) (2017).

[51] Heavy Flavor Averaging Group (HFLAV), http://www.slac.stanford.edu/xorg/hflav/charm/.

[52] M. Ablikim *et al.* (BESIII Collaboration), Chin. Phys. C **44**, 040001 (2020).

[53] E. Kou *et al.* (Belle II Collaboration), Prog. Theor. Exp. Phys. **2019**, 123C01 (2019).